FLEXIBLE CORE MASKING TECHNIQUE FOR BEAM HALO MEASUREMENTS WITH HIGH DYNAMIC RANGE

J. Egberts, S. Artikova, MPI-K, Heidelberg, Germany
C.P. Welsch, Cockcroft Institute, Warrington, Cheshire, UK, University of Liverpool, Liverpool, UK

Abstract

The majority of particles in a beam are located close to the beam axis, called the beam core. However, particles in the tail distribution of the transverse beam profile can never be completely avoided and are commonly referred to as beam halo.

The light originating from or generated by the particle beam is often used for non- or least destructive beam profile measurements. Synchrotron radiation, optical transition, or diffraction radiation are examples of such measurements. The huge difference in particle density between the beam core and its halo, and therefore the huge intensity ratio of the emitted light is a major challenge in beam halo monitoring.

In this contribution, results from test measurements using a flexible core masking technique are presented indicating way to overcome present limitations. This technique is well-known in e.g. astronomy, but since particle beams are not of constant shape in contrast to astronomical objects, a quickly adjustable mask generation process is required. The flexible core masking technique presented in this paper uses a micro mirror array to generate a mask based on an automated algorithm.

INTRODUCTION

The detection and possible control of the beam halo is of utmost importance for high energy accelerators, where unwanted particle losses lead to an activation or even damage of the surrounding vacuum chamber. But also in low-energy machines like the USR [1] one is interested in minimizing the number of particles in the tail region of the beam distribution. Since most part of the beam is normally concentrated in the central region, observation techniques with a high dynamic range are required to ensure that halo particles can be monitored with sufficient accuracy. One option to monitor the beam halo is to use light generated by the beam, either through synchrotron radiation (SR), optical transition radiation (OTR), or luminescent screens. In thus case, a special detection technique is required to allow for high dynamic range measurements.

The flexible core masking technique is based on the core masking technique which is well established in astronomy to observe the corona of the sun [2]. For an accurate image acquisition of the corona, an exposure time is required at which a normal camera overexposes due to the bright central region of the sun. The resulting blooming effects will superimpose the corona light and make an accurate image acquisition impossible. Therefore, the central bright region region of the sun is masked out to allow for a corona measurement without any negative blooming effects. The same principle can be applied for beam halo measurements, as already shown in [3, 4]. Test measurements of this kind have been performed at CERN by T. Lefèvre et al [5].

Unlike astronomical objects, an accelerator beam's profile is typically variable in shape. A technique using a fixed mask does not suffice any more and a flexible core masking technique is required. Taking advantage of the unique features of *Micro Mirror Arrays (MMA)*, flexible masks required for this technique become feasible.

MICRO MIRROR ARRAY

The *Micro Mirror Array* used for the measurements consists of an array of 1024×768 micro mirrors of 13.68μm×13.68μm size. Each of them can individually be set to $\pm 12^\circ$ [6]. Light will then be reflected in different directions depending on the micro mirror state. It is thereby possible to use the MMA as a reflective display which can be utilised as an adjustable mask.

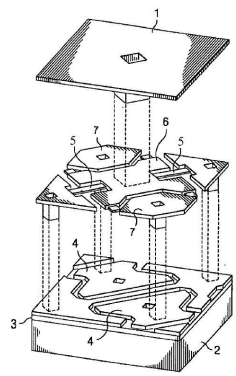

Figure 1: *MMA* Pixel Scheme [7].

Each single pixel of the *MMA* can be separated in a substructure and superstructure. The mirror itself is attached to the superstructure. The substructure of the pixels consists of a silicon substrate (fig.1-2) with an insulating layer (fig.1-3) on top, which isolates the superstructure from the substructure. Upon the insulating layer, there is a thin metallic layer, which forms the lower address electrodes (fig.1-4) and also supports the hinge. The hinge consists of the flexible torsion beam (fig.1-5), the large hinge yokes (fig.1-6), and upper address electrodes (fig.1-7).

If there is an appropriate potential applied to the upper and the lower electrodes (fig.1-4; 1-7), the electrostatic

force between them induces a torque and causes the hinge to tilt. The torsion beam (fig.1-5) acts as a torsion spring and creates a resisting torque. The hinge is tilted until the resisting torque of the torsion spring and the electrostatic torque are of the same magnitude or until it is stopped mechanically by touching the substructure. Since the pixel is used only in a digital ON-OFF mode, the voltage between the two electrodes is set high enough to cause the maximum deflection.

EXPERIMENTAL SETUP

We simulate a typical (Gaussian) distribution as it can be found in most particle beams, by using a conventional HeNe laser in our lab. The opening angle of the laser of 0.1° corresponds to SR/OTR emitted at some 100 MeV and can be regarded as a realistic approximation of a real particle beam.

The laser beam is reflected by an MMA into an 8Bit CCD-camera that measures the two dimensional beam profile, as illustrated in Fig. 2. If the mask is displayed on the MMA, the central beam core (red) will be deflected while the halo (blue) is still reflected into the CCD-camera. The challenge of measuring a high dynamic range is reduced to the issue a measuring a low intensity which can be done by increasing the exposure time of the camera or by removing neutral density filters that were included before.

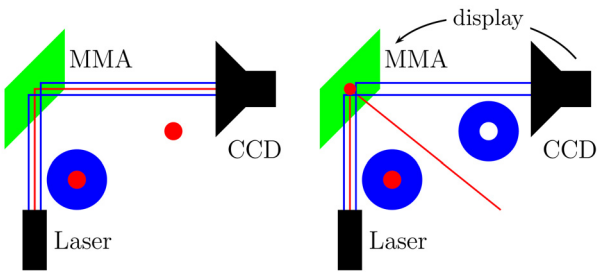

(a) Laser profile measurement (b) display beam core on MMA

Figure 2: After the profile is measured (a), its image (red) is displayed on the MMA to mask out the core to only reflect the halo into the camera (b).

MASK GENERATION

The mask is generated by displaying an image of the laser beam core on the *MMA*. Since the *MMA* is a digital device, the grey-scale image acquired by the CCD has to be transformed into a binary image. All pixels above a certain threshold are set to white, and all pixels below are set to black. The mask can then be stretched to the size that is required for the measurement.

The mask generation process consists therefore of three parts, the beam profile measurement, the conversion in a binary image, and the re-scaling of the mask to the desired size. To have a minimal negative effect of any light intensity fluctuations on the mask size during the image conversion, the threshold should be applied at the point of the maximum slope of the intensity distribution. On the other hand, as the mask is resized, the error of the mask shape also increases by the scaling factor. It can therefore be assumed that the total error of the mask is given by

$$\Delta M \propto \left(\frac{\partial I(x)}{\partial x}\right)^{-1} * R, \qquad (1)$$

with ΔM being the error of the mask shape, $I(x)$ being the light intensity distribution at threshold position x, and R being the scaling factor. Assuming a Gaussian shaped intensity distribution, ΔM is minimised by setting the first derivative to zero.

$$\frac{\partial}{\partial x}\left(x\frac{\partial}{\partial x}e^{-\frac{x^2}{2\sigma^2}}\right) = 0 \qquad (2)$$

This yields $x^2 = 2\sigma^2 \Rightarrow x = \sqrt{2}\sigma$. The threshold for setting the 8-Bit grey values to black or white is therefore chosen to be at $1/e$ of the maximum brightness. The highest brightness in an 8-Bit image is $2^8 - 1 = 255$ which gives a threshold of $255/e$.

To avoid an additional rescaling of the mask due to the diverging beam, the beam profile from which the mask is generated is acquired where the *MMA* is located.

MEASUREMENT

A control software was written that is able to control the CCD-camera and the *MMA*. It realises the mask generation and allows for a precise positioning of the mask on the *MMA*. The acquired two dimensional images are projected over 10 pixel rows to achieve a better statistics. Projections of various mask sizes are shown in Fig. 3.

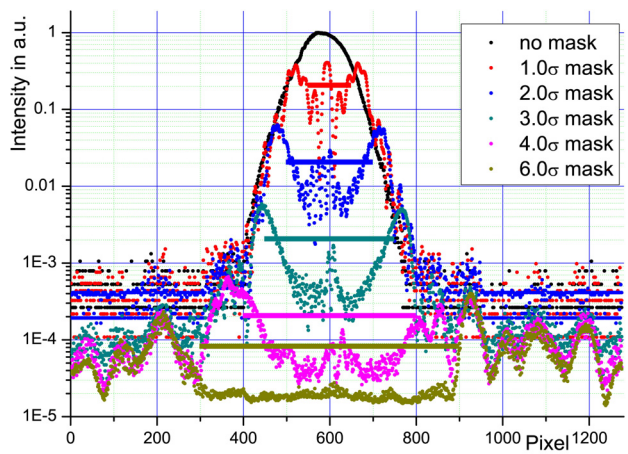

Figure 3: Projected profiles for various mask sizes.

To take full advantage of the 8Bit dynamic range of the CCD-camera, the exposure time is varied for each measurement to achieve an optimum result. In the analysis, the camera output therefore needs to be scaled by the exposure time to grant a quantity proportional to the light intensity.

The camera output was found to be highly linear with respect to the inverse exposure time.

In the central region a strong interference pattern is visible created by the mask. But for the beam halo observation this is of no further interest. In the outer halo region, some pattern is visible that is found to be part of the intrinsic laser beam profile.

Since the pattern outside the beam core is the major limitation to the achievable dynamic range, an iris is used to "cut off" this pattern. As the *MMA* and the mask can both generate interference patterns, the iris is carefully inserted in front of the *MMA* not to cut of any interference patterns caused by the *MMA*. Thereby, the dynamic range was calculated to be 1:300,000 which corresponds to 5.5 orders of magnitude.

Laser Correction

In the method described above, the mask always has to be smaller than the iris to observe a sensible signal. To overcome this limitation, a spatial mode filter can be used to generate a perfect Gaussian beam profile instead of cutting off the fringes.

The basic principle of a spatial mode filter is illustrated in Fig. 4. In the Fourier plane of the first lens, a pinhole is located to filter out higher orders and thereby generate the theoretically predicted Gaussian distribution of a laser beam.

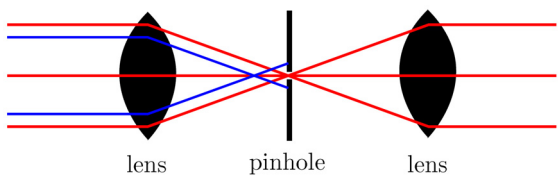

Figure 4: Principle of a spatial mode filter.

The major challenge of setting up the spatial mode filter is the high precision adjustment of the lenses and the pinhole. If the pinhole is misplaced in transverse direction, the beam profile is strongly distorted in one direction. By the use of micrometer screws, this positioning is done very precisely and its negative effects can almost be neglected. In case of a longitudinal misplacement of the pinhole, it is not exactly located in the Fourier plane of the focussing lens. The Fourier transform will still have a spatial component that creates an interference pattern when passing through the pinhole. The correct longitudinal adjustment of the pinhole mainly determines the dynamic range of the resulting Gaussian distribution of the laser beam.

The most reliable method of adjusting the spatial mode filter was achieved by first positioning the pinhole with respect to the first focussing lens. If the focal point of the lens matches the pinhole, the backscattered light between lens and pinhole will be at its minimum. The longitudinal and transversal position of the pinhole can thereby be adjusted very precisely. For the positioning of the second lens, a total focussing effect of the spatial mode filter must be avoided. It proved to be most accurate to focus the laser to a distant point.

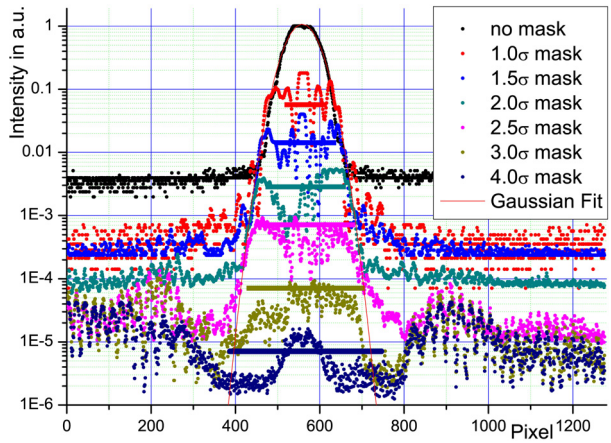

Figure 5: Projected profiles for various mask sizes for a laser beam corrected by a spatial mode filter.

It was possible to achieve a Gaussian shaped laser beam profile over more than four orders of magnitude, as indicated in Fig. 5. Based on this measurement, a dynamic range of six orders of magnitude is calculated.

CONCLUSION

The flexible core masking technique proved to be a reliable method for high dynamic range measurements of up to six orders of magnitude. The disadvantage of the flexible core masking technique is the complex setup and the lower dynamic range in comparison to other measurement techniques like the use of CID-cameras. On the other hand, this technique is a low budget alternative granting high dynamic ranges in short acquisition times.

REFERENCES

[1] C.P. Welsch, J. Ullrich et al., "An ultra-low-energy storage ring at FLAIR", Nucl. Instr. and Meth. A 546 (2005) 405417.

[2] B.R. Oppenheimer et al, "The Lyot Project: Status and Deployment Plans", AMOS Technical Conference, 2003

[3] C.P. Welsch, E. Bravin, B. Burel, T. Chapman, T. Lefèvre, M.J. Pilon, "Alternative Techniques for Beam Halo Measurements", Meas. Sci. Technol. 17 (2006) 2035c

[4] J. Egberts, S.Artikova, C.P. Welsch, E. Bravin, T. Lefèvre, T. Chapman, M.J. Pilon, "Design of a Beam Halo Monitor with Dynamic Range", TUP076, LINAC08, 2008, Victoria, Canada

[5] T. Lefèvre et al., "Beam Halo Monitoring at CTF3", THPLT147, Proc. EPAC 2004, 2004, Lucerne, Switzerland

[6] Texas Instruments, "DMD Discovery 1100 Conroller Board & Starter Kit", 2005

[7] T.J. Meyer AND B.A. Mangrun AND M.F. Reed, "Split Beam Micromirror", Texas Instruments Inc., 2006